Title

Intraoperative use of optical coherence tomography to differentiate normal and diseased thyroid and parathyroid tissues from lymph node and fat

Journal

Lasers in Medical Science, 36(2)

ISSN

0268-8921

Authors

Rubinstein, Marc
Hu, Allison C
Chung, Phil-Sang
et al.

Publication Date

2021-03-01

DOI

10.1007/s10103-020-03024-z

HHS Public Access

Author manuscript

Lasers Med Sci. Author manuscript; available in PMC 2022 March 05.

Published in final edited form as:

Lasers Med Sci. 2021 March ; 36(2): 269–278. doi:10.1007/s10103-020-03024-z.

Intraoperative use of Optical Coherence Tomography to differentiate normal and diseased thyroid and parathyroid tissues from lymph node and fat

Marc Rubinstein, MD[1,2,*], **Allison C Hu, BA**[1,2,3,*], **Phil-Sang Chung, MD**[4,5], **Jason H Kim, MD**[1], **Kathryn E Osann, PhD, MPH**[6], **Paul Schalch, MD**[1], **William B Armstrong, MD**[1], **Brian JF Wong, MD, PhD**[1,2,3]

[1]Departement of Otolaryngology – Head and Neck Surgery, University of California Irvine, Orange, California, USA

[2]Beckman Laser Institute and Medical Clinic, University of California Irvine, Irvine, California, USA

[3]Department of Biomedical Engineering, University of California Irvine, Irvine, California, USA

[4]Beckman Laser Institute Korea, Dankook University, Cheonan, Korea

[5]Department of Otolaryngology – Head and Neck Surgery, College of Medicine, Dankook University, Cheonan, Korea

[6]Department of Medicine, University of California Irvine, Orange, California, USA

Abstract

Purpose: The purpose of this study is twofold: 1) to determine the feasibility of optical coherence tomography (OCT) to differentiate normal and diseased tissue of the neck region intra-operatively, and 2) to evaluate how accurately a cohort of test subjects can identify various tissue types when shown a sample set of OCT images.

Methods: In this *in vivo*, prospective, single institutional study, an OCT imaging system (Niris, Imalux, Cleveland, OH) was used to image parathyroid, thyroid, lymph node, and fat tissue in 76 patients during neck surgery. Biopsies were performed for comparison of OCT images to histology in select cases (n=20). Finally, a group of either surgeons or scientists familiar with OCT (n=17) were shown a sample of OCT images and asked to identify the tissue.

Results: A total of 437 OCT images were analyzed and characteristic features of each tissue type were identified. OCT demonstrated distinct differences in structural architecture and signal intensity that differentiation between thyroid and parathyroid tissues, lymph nodes, and fat. OCT images were also compared with histology with good correlation. There was no difference in correctly identifying OCT imaged tissue type between surgeons and scientists.

Correspondence: Brian J.F. Wong, MD, PhD, Beckman Laser Institute and Medical Clinic University of California, Irvine, 1002 Health Sciences Rd Irvine, CA 92617, USA, bjwong@uci.edu, (714) 456-5753.

*The first two authors contributed equally to this work should be considered co-first authors

This work was presented at the American Academy of Otolaryngology—Head and Neck Surgery 2010 Annual Meeting

Conclusion: This study is the first *in vivo* OCT imaging study to evaluate both normal and diseased tissues that may be encountered during neck surgery. OCT has the otential to become a valuable intra-operative tool to differentiate diseased and normal thyroid tissue. intraoperatively to obtain an “optical biopsy” in real time without fixation, staining, or tissue resection.

Keywords

optical coherence tomography; OCT; thyroid; parathyroid; lymph node; head and neck; otolaryngology; oncology

Introduction

During neck surgery, it can be difficult to distinguish between thyroid, parathyroid, fat and lymph node tissue. Most endocrine surgeons agree that a diagnostic tool to aid in parathyroid detection intra-operatively would be incredibly beneficial as parathyroid glands are small and variable in their anatomical locations, rendering them at high risk for unintentional resection and subsequent hypoparathyroidism [1]. Temporary postoperative hypoparathyroidism has been shown to occur in 18% of cases and permanent postoperative hypoparathyroidism occur in 1.9% [2]. Postoperative hypoparathyroidism occurs as a result of parathyroid removal or ischemia and may be directly related to the surgeon’s capacity to detect and preserve the glad during the operation. Currently, the identification of parathyroid glands is particularly challenging and time consuming as they can be commonly confused with lymph nodes, adipose tissue, or extra-glandular thyroid tissue [1]. While many attempts have been made to visualize parathyroid glands intra-operatively using scintigraphy [3], staining agents [4], and fluorescence spectroscopy [5], none have been adopted for routine intraoperative use.

Optical coherence tomography (OCT) is a high-resolution microscopic imaging modality that combines a broadband, low-coherent light with interferometry to visualize living tissue microstructure [6, 7]. OCT works in a similar manner to ultrasound but uses near-infrared light instead of sound waves to distinguish intrinsic differences in tissue structures. In general, OCT systems can have an axial resolution of approximately 10μm with a depth penetration up to 2mm [8]. It generates cross-sectional images with high resolution, approaching that of light microscopy. OCT also has several medical applications, especially in ophthalmology [9], dermatology [10], oncology [11], and cardiology [12]. Quantitative analyses of OCT images have been demonstrated in dermatologic cancers such as melanoma [13], basal cell carcinoma [14], and squamous cell carcinoma [14], as well as ophthalmologic conditions [15]. In the head and neck, OCT has been used to image various anatomical regions, such as the tympanic membrane [16, 17], nasal cavity [18–20], oral cavity [21–23], airway [24–26], pediatric airway [27–29], larynx [8, 30–35], vocal chords [36–40], and cilia [41]. Most studies utilizing OCT to distinguish between normal thyroid, parathyroid, lymph node, and adipose tissue have been *ex vivo* studies [42–46], with only one study performed *in vivo* [47]. Recently, the first *ex vivo* study comparing these tissues in their pathological states was published [48]. However, to date, there are no *in vivo* studies evaluating the full spectrum of tissue types that may be encountered during neck surgery: from normal and diseased thyroid and parathyroid tissues to fat and lymph nodes.

Furthermore, the study of OCT imaging in neck surgery is at a critical juncture in translating from the laboratory to the clinic. Determining whether there are differences in OCT image interpretation of common neck tissues between scientists and clinicians would be valuable to enhance its translatable potential. Therefore, the purpose of this study is twofold: 1) to determine the feasibility of OCT to differentiate normal and diseased tissue of the neck region intra-operatively, and 2) to evaluate how accurately a group of physicians and OCT technology development researchers can correctly identify head and neck tissue types from OCT images alone.

Materials and Methods

Study Design

This is a prospective single-institution *in vivo* study that was approved by the institutional review board. Informed consent was obtained from all patients. OCT imaging was performed in patients undergoing neck surgery at the University of California Irvine Medical Center.

OCT System and Imaging

A previously described portable commercial time-domain OCT system (Niris, Imalux Corporation, Cleveland, Ohio, USA) was used for all images (Fig. 1A) [17]. This OCT system uses low-coherent broadband, near-infrared light with a central wavelength of 1,310nm to acquire real-time images of 200 × 200 pixels at a maximum frame rate of 0.7 Hz. Images are acquired at a lateral resolution of 25μm (diffraction limited) and axial resolution of 10 to 20μm. The lateral scanning range is 1.5 to 2.5mm and the depth scanning range is 2.2mm. A multi-use flexible probe (2.7mm in diameter, 2M long), containing a single mode fiber raster scanned by a solenoid across the surface of a grin lens, was used to acquire images (Fig. 1B).

Imaging was performed intra-operatively. The imaging probe was sterilized prior to each procedure using either autoclave or the Steris system and covered with a sterile plastic sheath. After the desired tissue in the neck was surgically exposed, the tip of the sterilized probe was place in light contact with the tissue of interest. Images of the multiple structures in the neck were obtained in less than 5 minutes in each subject at a frame rate of 1Hz and resolution of ~10μm with a 1mm depth penetration. The OCT system monitor displays real-time images that allow the surgeon to receive immediate feedback, similar to ultrasound. None of the information obtained during imaging was used to inform clinical decision making. Imaging characteristics of each tissue type were identified and summarized (Table 1).

Histopathology

When clinically indicated, intra-operative biopsies of suspected parathyroid tissue and lymph nodes were also obtained and sent for frozen section and/or permanent histology (n=20). Specimens sent for permanent histopathology were fixed in 10% buffered formalin, embedded in paraffin wax and cut at 4 to 5μm for hematoxylin and eosin. The slides were

examined and photographed at magnifications of 100 to 200x, to approximate the field of view of the OCT system.

OCT and Histopathology Correlation

OCT images of each tissue type were grouped and compared with histological stains of the respective tissue type. Representative OCT images and histological sections for each tissue type were then selected based on the shape and size of hallmark structures such as cells, fat, follicles, nodules, and capsules to ensure comparable features between the two types of images.

Cohort Analysis

A group of 17 participants, consisting of 10 surgeons and 7 scientists, were included. Surgeons consisted of residents and attending physicians in either general surgery or otolaryngology. The scientist cohort included lab research engineers with expertise in OCT technology but did not have a background in clinical pathology of head and neck organs. We chose to survey both surgeons and OCT scientists in order to evaluate whether there would be a substantial difference in image identification between those familiar with the disease process and those familiar with technology development.

A three-part digital questionnaire was created (SurveyMonkey, San Mateo, California, USA). Part one consisted purely of OCT images of normal and diseased parathyroid, thyroid, lymph node and fat tissues without their counterpart histological stains. The correct answers were presented on the second page, with a short explanation of features and criteria used to differentiate these tissues. In part two, a short tutorial was presented, showing the characteristic features of each tissue type (summarized in Table 1). This tutorial was used to educate participants of the differences in tissue architecture of the thyroid, parathyroid, lymph node and fat tissues and the diagnostic OCT criteria used to identify each tissue type. In part three, participants were presented with 32 OCT images and asked to identify whether the OCT images were normal thyroid, nodular thyroid, thyroid cancer, normal parathyroid, parathyroid adenoma, lymph node, or fat.

Statistical Analysis

Chi-square was used to determine differences in correctly identifying each tissue type between scientists and surgeons. P-value <0.05 was considered significant.

Results

A total of 437 OCT images were acquired in 76 patients (male, 40.8%) undergoing thyroid, parathyroid, or neck dissection operations (Fig. 2). The mean age was 30 years old (range, 15–80 years). There were 69 images of normal thyroid, 41 images of thyroid nodules, and 11 images of thyroid cancer. There were 119 images of normal parathyroid, 34 images of parathyroid adenoma, 111 images of lymph node tissue, and 28 images of fat taken from 72 patients.

The first objective of this study was to visually correlate OCT images with histopathology and to identify diagnostic OCT criteria for the various pathologic diagnoses made using light microscopy. The different OCT features between the pathological tissue types and the normal tissues were characterized (Table 1).

A second objective of this study was also to analyze how accurately a cohort of scientists and surgeons were able to identify tissue types based on OCT images. A total of 32 OCT images were chosen for analysis. These images were high quality photos that were not used as part of the figures presented in this article. There were three images of normal thyroid, thyroid nodule, and thyroid cancer each. There were ten images of normal parathyroid tissue and nine images of parathyroid adenoma tissue, and two images of both lymph node tissue and fat (Table 2).

Thyroid Tissue

Distinctive characteristics of normal thyroid tissue in OCT imaging include a thin, high intensity capsule, and numerous large, lower intensity ovoid follicles in the subcapsular space (Fig. 3A). Histopathology similarly demonstrated relatively uniform colloid-filled follicles lined by a single layer of epithelial cells (Fig. 3B).

The architectural changes of benign lesions, such as a multi-nodular goiter, can also be observed under OCT. These changes include a thickened capsule of high intensity as well as enlargement of the low intensity thyroid follicles (Fig. 3C). Histology imaging also revealed a fibrous and calcified capsule containing enlarged thyroid follicles of varying sizes (Fig. 3D).

Cancerous thyroid tissues could also be identified using the OCT images. Distinguishing features of thyroid cancer cells include a thickened capsule with loss of low intensity follicles in the subcapsular space (Fig. 3E). Histopathology showed similar absence of thyroid follicles (Fig. 3F).

Parathyroid Tissue

Parathyroid tissue was found to have characteristic findings on OCT imaging that is readily distinguishable from thyroid, lymph nodes, and fatty tissue. OCT imaging of normal parathyroid tissue demonstrates a characteristically thin, high intensity capsule with small low intensity ovoid fat cells (Fig. 3G). Histology imaging demonstrated nests and cords of parathyroid cells with intervening stromal fat (Fig. 3H).

Parathyroid adenomas on the other hand appear more homogenous with increased cellularity of cells and decreased to absent fat cells (Fig. 3I). The increased cellularity of cells in the parathyroid adenomas is characterized by the lack of sharp transitional layer between the capsule and other layers. The high cellularity and lack of fat cells in the parathyroid adenoma was correlated in histopathology (Fig. 3J)

Lymph Nodes

Additional OCT imaging was performed in other anatomical structures such as normal lymph nodes. Similar to normal parathyroid glands and in contrast to normal thyroid tissue,

lymph node tissues have a homogenous layer of bright scattering intensity that slowly transitions to regions of lower signal intensity in the subcapsular space on OCT imaging (Fig. 3K-i). The lymph node capsule is of high signal intensity (Fig. 3K-ii) with an overlying layer of fat on the external surface (Fig. 3K-iii). The OCT images of normal lymph nodes were well correlated with histopathology as seen in Figure 3K, L. However, the follicles that are seen on histological staining are difficult to appreciate on OCT imaging (Fig. 3L-i).

Adipose Tissue

On OCT images, normal adipose tissue demonstrates a typical “honey-comb” like pattern, consisting of multiple low intensity ovoid pockets with a highly scattering framework of collagen fibers surrounding the lipid pockets (Fig. 3M). Histopathology demonstrated empty vacuoles separated by delicate fibrovascular septa producing a similar “honey-comb” appearance (Fig. 3N).

Cohort Analysis

In the surgeon group, there was a high percent correct in identifying normal thyroid tissue (80.0%), thyroid nodule (80.0%), and thyroid cancer (100.0%) (Table 2). This trend was also seen in the scientist group, where correct identification of normal thyroid tissue, thyroid nodule, and thyroid cancer were 85.7%, 90.5%, and 100.0% respectively. The correct identification of normal parathyroid, parathyroid adenoma, fat and lymph nodes were 50.0%, 64.4%, 30.0%, and 50.0%, respectively among surgeons. Scientists also scored similarly in the non-thyroid tissues: 55.7%, 74.6%, 35.7%, and 64.3%, respectively. There were no differences in correct identification of each tissue type between the scientists and surgeons, and the differences in scores were due to individual variability (Table 2).

The average correct identification of normal thyroid tissue, thyroid nodule, and thyroid cancer were 82.4%, 84.3%, and 100.0%, respectively among surgeons and scientists combined (Figure 4). The correct identification of normal parathyroid, parathyroid adenoma, fat and lymph nodes were 52.3%, 68.6%, 55.9%, and 32.4% respectively among surgeons and scientists combined. Overall, there was high accuracy in distinguishing diseased thyroid tissue from normal thyroid tissue.

Discussion

In this study we used OCT to image thyroid, parathyroid, lymph node, and fat tissue during thyroid surgery and neck dissections with the goal of identifying the features that would aid in tissue characterization. We also evaluated how accurately a group of physicians and OCT technology development researchers could correctly identify tissue types from OCT images alone. OCT demonstrated adequate image quality and distinct differences in structural architecture and signal intensity that allowed adequate differentiation between thyroid and parathyroid tissues, lymph nodes, and fat. When available, OCT images were compared with histology with good correlation. When participants were asked to identify tissue types based on OCT images alone, there was high accuracy in distinguishing between normal thyroid and either nodular or cancerous diseased thyroid tissue. However, participants had difficulty differentiating parathyroid tissue from lymph node tissue and fat.

Previous reports have demonstrated that OCT can be used to identify characteristic structural features for thyroid, parathyroid, lymph node and adipose tissue both *ex vivo* and *in vivo* [42–48]. Pantanowitz et al used high-resolution OCT to differentiate normal thyroid from pathological processes from the thyroid, and were able to identify changes in the thyroid in different benign and malignant pathologies [42]. Zhou et al used a combined OCT and Optical Coherence Microscopy (OCM) system to image benign and malignant thyroid lesions and identified key elements of each of the different lesions, which were successfully correlated with histology [43]. In a similar study, McLaughlin et al used OCT to identified microstructural changes in both benign and metastatic lymph nodes, and were accurately correlated with histology [11]. In an *ex vivo* pilot study by Conti de Freitas et al and an *in vivo* study by Sommerey et al, characteristic OCT imaging features of each tissue type (thyroid, parathyroid, lymph nodes, fat) in its normal state were presented, which were similarly seen in our study (Table 1) [45, 47]. In contrast to prior studies, our study provides the first *in vivo* OCT imaging analysis to identify and evaluate both normal and diseased thyroid and parathyroid tissue intra-operatively [49]. The possibility of diagnosing tissue pathology intraoperatively using an OCT device would have widespread applications in neck operations and would reduce the reliance upon frozen section biopsy of tissues. Only those lesions suspect for a given pathology will need to be operatively biopsied for confirmation.

OCT imaging was able to demonstrate distinct differences in structural architecture and signal intensity that allowed us to differentiate between thyroid and parathyroid tissues, lymph nodes, and fat. Thyroid tissue was clearly seen using OCT. Normal thyroid tissue has an architecture made up of follicles, round to slightly oval structures lined by a single layer of cells, with lumens containing colloid. Distinctive characteristics seen in thyroid tissue under microscopic examination were also seen using OCT (Fig. 3A, B).

Benign lesions such as a multinodular goiter also show architectural changes including multiple nodules of thyroid follicles of varying size, as well as fibrosis and calcification. These changes were also seen on OCT as a thickening of the thyroid capsule with enlargement of the thyroid follicles (Fig. 3C, D). When comparing normal thyroid to thyroid nodules, normal thyroid tissue was characterized by a thin layer of high intensity capsule with low intensity follicles, whereas thyroid nodules showed a thicker layer of high intensity capsule with low intensity follicles (Fig. 3A, C). However, the increase in the capsule thickness was not always evident or clearly thickened compared to the normal thyroid tissues. This made it slightly more difficult to correctly distinguish normal thyroid and thyroid nodules consistently. Finally, OCT imaging of thyroid cancer presented a thick layer of high intensity capsule with loss of the low intensity follicles in the subcapsular space (Fig. 3E).

Parathyroid tissue was found to have characteristic findings on OCT imaging that is readily distinguishable from thyroid, lymph nodes, and fatty tissue. Normal parathyroid tissue is made up of chief cells and oxyphil cells in varying proportions, separated by variable amounts of stromal fat. On OCT imaging, normal parathyroid tissues were populated by spots of low signal intensity in the subcapsular region indicative of known fatty deposits. Parathyroid adenomas can be differentiated from normal parathyroid tissue by evidence of

decreased fat cells and increased cellularity in the subcapsular space (Fig 3G, I). These are subtle differences that are difficult to identify consistently and accurately.

In lymph nodes, the most obvious structures are the follicles, generally rounded in appearance. These follicles are mainly present in the cortical area, which is the outer area of the lymph node, just below the fibrous capsule. Although the follicular structures in the outer cortex of lymph nodes can be seen on histology, they are poorly visible on OCT imaging (Fig. 3K, L). This lack of distinction makes it more difficult to distinguish lymph node from parathyroid tissues on OCT imaging. Therefore, while normal and diseased thyroid tissues were more easily differentiated on OCT imaging, it was more difficult to differentiate between normal parathyroid glands, parathyroid adenomas, and lymph nodes as all these tissues contain a thin capsule (Fig. 3G–K). Furthermore, when the parathyroid tissue is compared to adipose tissue (Fig. 3G, M), clear differences are seen. The normal adipose tissue is made up of lobules of relatively uniform adipocytes, which appear clear since most of the cell is occupied by a single lipid-filled cytoplasmic vacuole.

Overall, we demonstrated that OCT can be used as a tool to differentiate parathyroid tissue from fat and other structures during endocrine surgery. The distinguishing OCT imaging findings of the parathyroid tissue is the vacuolated appearance of the adipocytes within the capsule. Other key element is the lack or very thin capsule of the parathyroid when compared to a lymph node, which has a thicker capsule.

When participants were asked to identify tissue types based on OCT images alone, there was high accuracy of differentiation between normal thyroid and either nodular or cancerous diseased thyroid tissue. In contrast, participants had difficulty differentiating parathyroid tissue from lymph node tissue and fat. It is still important to note that although OCT characteristics can be easily taught, there is still a short learning curve in learning how to correctly identify the tissue types. The investigator (M.R.) who analyzed the initial OCT images from the 76 patients noted that the ability to accurately identify parathyroid and lymph node tissue only began after analyzing about 20 patient cases. This suggests that experience in looking at OCT images is still an important factor to how accurately an individual can identify tissues based on OCT images. Overall, OCT imaging device use and image analysis can be easily taught to educated professionals, and accuracy of tissue identification increases with experience in looking at OCT images. This suggests that if the OCT imaging device were approved for use in the clinical setting, it has the potential to be quickly adopted due to its portability, ease of operation, and ease in image interpretation. Some basic, not intensive, training is required for use or for interpretation.

When comparing the accuracy of identifying tissue types between the surgeons and scientists, there was no significant difference. It is important to note that the only difference between physicians and researchers is that the physicians had a background to the pathology of the disease. However, the lack of significance between rates of correct tissue identification between surgeons and scientists suggests that knowing the pathology of the disease may not be an important factor in reading OCT images. Perhaps correct identification relies more on pattern recognition rather than medical background. This is important because this means that once prototypical features of each tissue type can be well

characterized, they can be easily taught to clinicians or another educated audience who are new to the technology. A highly specialized medical background is not required for OCT imaging, and its potential applicability could be expanded to a broader audience to include general surgeons who are not highly specialized in endocrine surgery. Of note, our survey groups were relatively few in number and there were unequal subjects in each subgroup, which may limit the applicability of the accuracy of our results to a broader population.

OCT is a portable imaging modality that uses near-infrared light interferometry to obtain high-resolution (1–20μm) images of the internal microstructure of bio-tissue non-invasively and non-destructively. With the ability to image in cross-sectional and volumetric orientations, OCT can provide similar information as histological analysis, such as spatial, locational, and structural details. Taken together with its non-invasive design, OCT has great potential to replace biopsies and pathology examination with a real-time “optical biopsy.”

There are some similarities that can be drawn between OCT and ultrasound, a common imaging modality used for detecting thyroid pathology. Both OCT and ultrasound are non-invasive devices that produce images of high quality. However, OCT produces images using a near-infrared light source rather than sound waves used in ultrasound. In addition, because light waves travel faster (3×108m/s) than sound waves (approximately 1500 m/s), OCT image resolution (10μm) is much higher than that of ultrasound (150μm), and therefore has the potential to differentiate tissue microstructures, not just gross anatomical structures. In recent years, we have seen a greater use of bedside ultrasounds in the diagnosis of disease and its assistance in bedside procedures [50]. With adequate improvements in OCT technology, OCT imaging device adoption into clinical practice may follow a path similar to that of ultrasound technologies and ultimately become a point of care device available in all operating rooms.

Importantly, OCT imaging has a limited penetration depth of only 2mm. It evaluates only the superficial layers of tissues, and in some cases may provide false readings due to tissue samples being surrounded by adipose tissue. This may cause false identification of tissue types is the specific tissue of interest is surrounded by a fat layer. In addition, the resolution of the commercial OCT Imalux system is below that of contemporary research devices, and therefore, improvements in technology development is still needed for better image resolution in the portable commercial system. However, OCT is still a very useful imaging tool in that it provides valuable information about tissue architecture that is useful in distinguishing various tissue types from one another as shown by this article.

Current standard to identify parathyroid glands intra-operatively is via frozen sections. There is time delay needed to biopsy, process tissues, embed and stain, and then finally have the slides read by a pathologist. Additionally, it is tedious and potentially impossible to also inspect all the surrounding tissues. Non-invasive methods include the float and sink method or the use of staining agents, both of which can be inaccurate and cause adverse effects. OCT imaging would augment a surgeon’s capabilities to correctly identify neck structures intraoperatively with less reliance of biopsying tissues that may cause unnecessary trauma and sacrifice of part of the tissue of interest. The target users of the OCT imaging device are endocrine specialists; however, it can also aid general surgeons in rural areas in performing

thyroid and parathyroid surgery. OCT has the potential to eventually become a point of care device that can elevate the expertise of general surgeons to a similar level as that of endocrine specialists in intra-operatively identifying correct tissue types for resection. In addition, OCT imaging is a portable commercial device that can be easily operated and may aid physicians who are interested in international medical mission trips to perform thyroid and parathyroid surgery.

In summary, OCT imaging has the potential to be a valuable intra-operative diagnostic tool that provides information in real-time. Identifying tissue types in real-time in the OR is a significant improvement to obtaining biopsies of tissues for histology. Further advances in improving OCT resolution and quality may allow OCT to become the new standard in identifying thyroid and parathyroid tissues intraoperatively to obtain an “optical biopsy” in real-time without resection, fixation, and staining. The adoption of OCT imaging in surgery may become a significant improvement in the practice of point of care medicine.

Conclusions

This is the first study to systematically use OCT to non-invasively image and differentiate normal and diseased parathyroid tissue from other neck structures *in vivo*. Further advances in improving OCT resolution, quality, and imaging depth may allow OCT to be used as an intraoperative tool to correctly identify and differentiate tissue types in real-time and potentially obviate the need for frozen section confirmation.

Acknowledgements

This work was supported by the National Institutes of Health (DC 006026, CA 91717, EB 00293, RR 01192, RR00827), Flight Attendant Medical Research Institute (32456), State of California Tobacco Related Disease Research Program (12RT-0113), Air Force Office of Scientific Research (F49620_00_1_0371), and the Arnold and Mabel Beckman Foundation.

REFERENCES

1. Thompson NW, Eckhauser FE, Harness JK (1982) The anatomy of primary hyperparathyroidism. Surgery 92:814–21 [PubMed: 7135202]
2. Ritter K, Elfenbein D, Schneider DF, et al. (2015) Hypoparathyroidism after total thyroidectomy: incidence and resolution. J Surg Res 197:348–353. 10.1016/j.jss.2015.04.059 [PubMed: 25982044]
3. Damadi A, Harkema J, Kareti R, Saxe A (2007) Use of pre-operative Tc99m-Sestamibi scintigraphy and intraoperative parathyroid hormone monitoring to eliminate neck exploration in mediastinal parathyroid adenocarcinoma. J Surg Educ 64:108–12. 10.1016/j.jsurg.2006.10.005 [PubMed: 17462212]
4. Derom AF, Wallaert PC, Janzing HM, Derom FE (1993) Intraoperative identification of parathyroid glands with methylene blue infusion. Am J Surg 165:380–2. 10.1016/s0002-9610(05)80850-5 [PubMed: 7680546]
5. McWade MA, Paras C, White LM, et al. (2013) A novel optical approach to intraoperative detection of parathyroid glands. Surgery 154:1371–1377. 10.1016/j.surg.2013.06.046 [PubMed: 24238054]
6. Huang D, Swanson E, Lin C, et al. (1991) Optical coherence tomography. Science (80-) 254:1178–1181. 10.1126/science.1957169
7. Fujimoto JG, Brezinski ME, Tearney GJ, et al. (1995) Optical biopsy and imaging using optical coherence tomography. Nat Med 1:970–972. 10.1038/nm0995-970 [PubMed: 7585229]

8. Wong BJF, Jackson RP, Guo S, et al. (2005) In vivo optical coherence tomography of the human larynx: normative and benign pathology in 82 patients. Laryngoscope 115:1904–11. 10.1097/01.MLG.0000181465.17744.BE [PubMed: 16319597]
9. Hirano K, Ito Y, Suzuki T, et al. (2001) Optical Coherence Tomography for the Noninvasive Evaluation of the Cornea. Cornea 20:281–289. 10.1097/00003226-200104000-00009 [PubMed: 11322417]
10. Welzel J (2001) Optical coherence tomography in dermatology: a review. Skin Res Technol 7:1–9 [PubMed: 11301634]
11. McLaughlin RA, Scolaro L, Robbins P, et al. (2010) Imaging of Human Lymph Nodes Using Optical Coherence Tomography: Potential for Staging Cancer. Cancer Res 70:2579–2584. 10.1158/0008-5472.CAN-09-4062 [PubMed: 20233873]
12. Kala P, Cervinka P, Jakl M, et al. (2018) OCT guidance during stent implantation in primary PCI: A randomized multicenter study with nine months of optical coherence tomography follow-up. Int J Cardiol 250:98–103. 10.1016/j.ijcard.2017.10.059 [PubMed: 29079414]
13. Turani Z, Fatemizadeh E, Blumetti T, et al. (2019) Optical Radiomic Signatures Derived from Optical Coherence Tomography Images Improve Identification of Melanoma. Cancer Res 79:2021–2030. 10.1158/0008-5472.CAN-18-2791 [PubMed: 30777852]
14. Adabi S, Hosseinzadeh M, Noei S, et al. (2017) Universal in vivo Textural Model for Human Skin based on Optical Coherence Tomograms. Sci Rep 7:17912. 10.1038/s41598-017-17398-8 [PubMed: 29263332]
15. Garcia Garrido M, Beck SC, Mühlfriedel R, et al. (2014) Towards a quantitative OCT image analysis. PLoS One 9:. 10.1371/journal.pone.0100080
16. Djalilian HR, Ridgway J, Tam M, et al. (2008) Imaging the Human Tympanic Membrane Using Optical Coherence Tomography In Vivo. Otol Neurotol 29:1091–1094. 10.1097/MAO.0b013e31818a08ce [PubMed: 18957904]
17. Djalilian HR, Rubinstein M, Wu EC, et al. (2010) Optical coherence tomography of cholesteatoma. Otol Neurotol 31:932–5 [PubMed: 20684054]
18. Mahmood U, Ridgway J, Jackson R, et al. In vivo optical coherence tomography of the nasal mucosa. Am J Rhinol 20:155–9 [PubMed: 16686378]
19. Englhard AS, Wiedmann M, Ledderose GJ, et al. (2018) In vivo imaging of the internal nasal valve during different conditions using optical coherence tomography. Laryngoscope 128:E105–E110. 10.1002/lary.26962 [PubMed: 29044537]
20. Englhard AS, Wiedmann M, Ledderose GJ, et al. (2016) Imaging of the internal nasal valve using long-range Fourier domain optical coherence tomography. Laryngoscope 126:E97–E102. 10.1002/lary.25785 [PubMed: 26599137]
21. Jerjes W, Upile T, Conn B, et al. (2010) In vitro examination of suspicious oral lesions using optical coherence tomography. Br J Oral Maxillofac Surg 48:18–25. 10.1016/j.bjoms.2009.04.019 [PubMed: 19726114]
22. Ridgway JM, Armstrong WB, Guo S, et al. (2006) In Vivo Optical Coherence Tomography of the Human Oral Cavity and Oropharynx. Arch Otolaryngol Neck Surg 132:1074. 10.1001/archotol.132.10.1074
23. Wang Y, Bachman M, Li G-P, et al. (2005) Low-voltage polymer-based scanning cantilever for in vivo optical coherence tomography. Opt Lett 30:53–5. 10.1364/ol.30.000053 [PubMed: 15648635]
24. Kimbell JS, Basu S, Garcia GJM, et al. (2019) Upper airway reconstruction using long-range optical coherence tomography: Effects of airway curvature on airflow resistance. Lasers Surg Med 51:150–160. 10.1002/lsm.23005 [PubMed: 30051633]
25. Jing JC, Chou L, Su E, et al. (2016) Anatomically correct visualization of the human upper airway using a high-speed long range optical coherence tomography system with an integrated positioning sensor. Sci Rep 6:39443. 10.1038/srep39443 [PubMed: 27991580]
26. Jing J, Zhang J, Loy AC, et al. (2012) High-speed upper-airway imaging using full-range optical coherence tomography. J Biomed Opt 17:110507 [PubMed: 23214170]
27. Ridgway JM, Ahuja G, Guo S, et al. (2007) Imaging of the Pediatric Airway Using Optical Coherence Tomography. Laryngoscope 117:2206–2212. 10.1097/MLG.0b013e318145b306 [PubMed: 18322424]

28. Ridgway JM, Su J, Wright R, et al. (2008) Optical coherence tomography of the newborn airway. Ann Otol Rhinol Laryngol 117:327–34 [PubMed: 18564528]
29. Lazarow FB, Ahuja GS, Chin Loy A, et al. (2015) Intraoperative long range optical coherence tomography as a novel method of imaging the pediatric upper airway before and after adenotonsillectomy. Int J Pediatr Otorhinolaryngol 79:63–70. 10.1016/j.ijporl.2014.11.009 [PubMed: 25479699]
30. Armstrong WB, Ridgway JM, Vokes DE, et al. (2006) Optical Coherence Tomography of Laryngeal Cancer. Laryngoscope 116:1107–1113. 10.1097/01.mlg.0000217539.27432.5a [PubMed: 16826043]
31. Sepehr A, Armstrong WB, Guo S, et al. (2008) Optical coherence tomography of the larynx in the awake patient. Otolaryngol Neck Surg 138:425–429. 10.1016/j.otohns.2007.12.005
32. Kraft M, Glanz H, von Gerlach S, et al. (2008) Clinical value of optical coherence tomography in laryngology. Head Neck 30:1628–1635. 10.1002/hed.20914 [PubMed: 18767182]
33. Coughlan CA, Chou L, Jing JC, et al. (2016) In vivo cross-sectional imaging of the phonating larynx using long-range Doppler optical coherence tomography. Sci Rep 6:22792. 10.1038/srep22792 [PubMed: 26960250]
34. Rubinstein M, Fine EL, Sepehr A, et al. (2010) Optical coherence tomography of the larynx using the Niris system. J Otolaryngol Head Neck Surg 39:150–6 [PubMed: 20211101]
35. Guo S, Yu L, Sepehr A, et al. (2009) Gradient-index lens rod based probe for office-based optical coherence tomography of the human larynx. J Biomed Opt 14:014017. 10.1117/1.3076198 [PubMed: 19256705]
36. Burns JA, Kim KH, Kobler JB, et al. (2009) Real-time tracking of vocal fold injections with optical coherence tomography. Laryngoscope 119:2182–6. 10.1002/lary.20654 [PubMed: 19676103]
37. Burns JA, Zeitels SM, Anderson RR, et al. (2005) Imaging the Mucosa of the Human Vocal Fold with Optical Coherence Tomography. Ann Otol Rhinol Laryngol 114:671–676. 10.1177/000348940511400903 [PubMed: 16240928]
38. Yu L, Liu G, Rubinstein M, et al. (2009) Office-based dynamic imaging of vocal cords in awake patients with swept-source optical coherence tomography. J Biomed Opt 14:064020. 10.1117/1.3268442 [PubMed: 20059258]
39. Guo S, Hutchison R, Jackson RP, et al. (2006) Office-based optical coherence tomographic imaging of human vocal cords. J Biomed Opt 11:030501. 10.1117/1.2200371
40. Vokes DE, Jackson R, Guo S, et al. (2008) Optical Coherence Tomography— Enhanced Microlaryngoscopy: Preliminary Report of a Noncontact Optical Coherence Tomography System Integrated with a Surgical Microscope. Ann Otol Rhinol Laryngol 117:538–547. 10.1177/000348940811700713 [PubMed: 18700431]
41. Jing JC, Chen JJ, Chou L, et al. (2017) Visualization and Detection of Ciliary Beating Pattern and Frequency in the Upper Airway using Phase Resolved Doppler Optical Coherence Tomography. Sci Rep 7:8522. 10.1038/s41598-017-08968-x [PubMed: 28819309]
42. Pantanowitz L, Hsiung P-L, Ko TH, et al. (2004) High-resolution imaging of the thyroid gland using optical coherence tomography. Head Neck 26:425–434. 10.1002/hed.10392 [PubMed: 15122659]
43. Zhou C, Wang Y, Aguirre AD, et al. (2010) Ex vivo imaging of human thyroid pathology using integrated optical coherence tomography and optical coherence microscopy. J Biomed Opt 15:016001. 10.1117/1.3306696 [PubMed: 20210448]
44. Ladurner R, Hallfeldt KKJ, Al Arabi N, et al. (2013) Optical coherence tomography as a method to identify parathyroid glands. Lasers Surg Med 45:654–659. 10.1002/lsm.22195 [PubMed: 24249200]
45. Conti de Freitas LC, Phelan E, Liu L, et al. (2013) Optical coherence tomography imaging during thyroid and parathyroid surgery: A novel system of tissue identification and differentiation to obviate tissue resection and frozen section. Head Neck 36:n/a-n/a. 10.1002/hed.23452
46. Hou F, Yu Y, Liang Y (2017) Automatic identification of parathyroid in optical coherence tomography images. Lasers Surg Med 49:305–311. 10.1002/lsm.22622 [PubMed: 28129441]

47. Sommerey S, Al Arabi N, Ladurner R, et al. (2015) Intraoperative optical coherence tomography imaging to identify parathyroid glands. Surg Endosc 29:2698–2704. 10.1007/s00464-014-3992-x [PubMed: 25475518]

48. Yang N, Boudoux C, De Montigny E, et al. (2019) Rapid head and neck tissue identification in thyroid and parathyroid surgery using optical coherence tomography. Head Neck hed 25972. 10.1002/hed.25972

49. Armstrong WB, Naemi K, Keel S, et al. (2010) Intraoperative Use of OCT in Endocrine Surgery. Otolaryngol Neck Surg 143:P63–P63. 10.1016/j.otohns.2010.06.075

50. Tyshlek D, Aubry J-F, Ter Haar G, et al. (2014) Focused ultrasound development and clinical adoption: 2013 update on the growth of the field. J Ther ultrasound 2:2. 10.1186/2050-5736-2-2 [PubMed: 25512866]

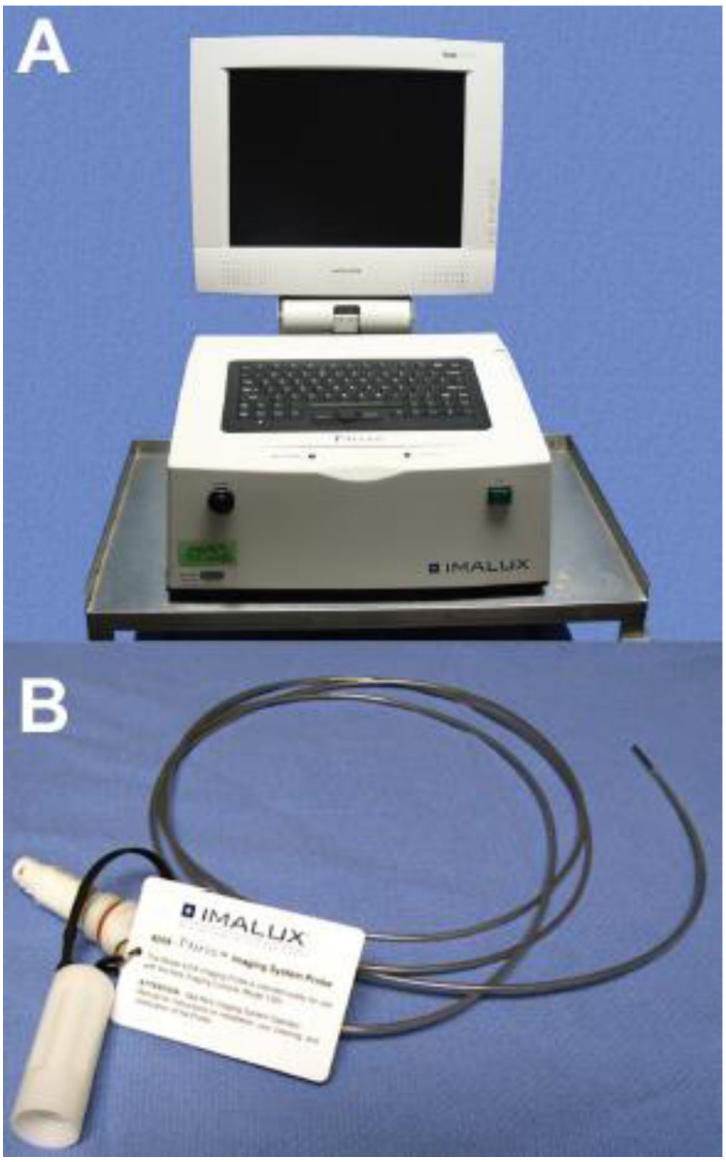

Figure 1.
A) Imalux Niris OCT Imaging System. B) 2.7mm diameter by 5M length flexible probe.

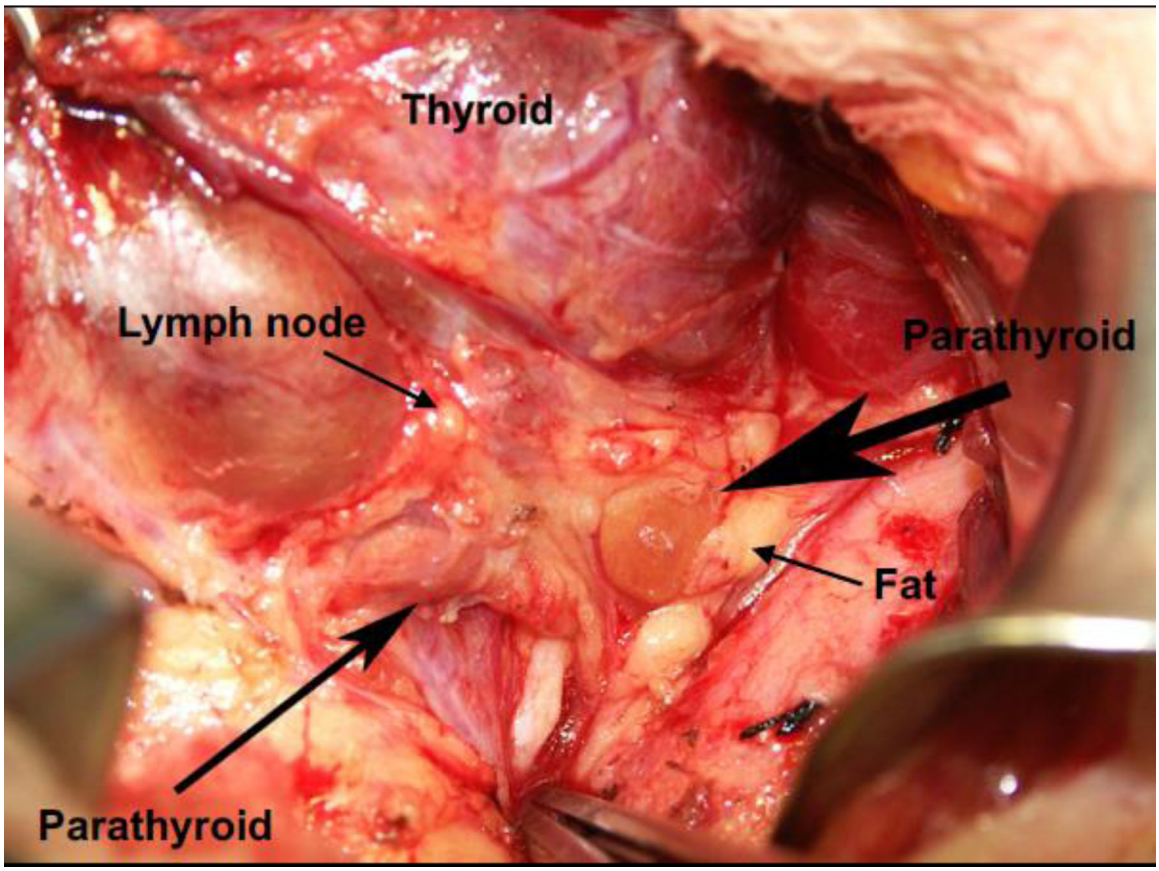

Figure 2.
Anatomical structures in the neck region.

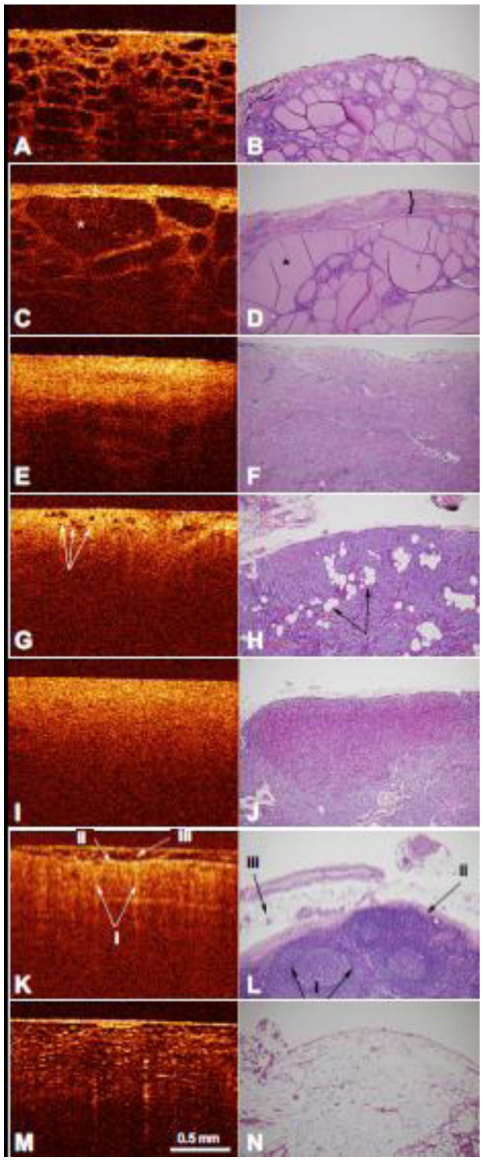

Figure 3.

A) OCT image of normal thyroid tissue with the corresponding histology (B). C) OCT image of multinodular thyroid tissue with enlargement of the thyroid capsule (indicated by the bracket) and thyroid follicle (indicated by the asterisk). D) Corresponding histology of multinodular thyroid tissue with a fibrous capsule (indicated by the bracket) and multiple nodules of thyroid follicles of varying size (indicated by the asterisk). E) OCT image of thyroid cancer with the corresponding histology (F). G) OCT image of normal parathyroid tissue with normal fat within the parathyroid tissue (indicated by arrows) and the corresponding histology (H) with nests and cords of parathyroid cells and intervening stromal fat (indicated by arrows). I) OCT image of parathyroid adenoma tissue with the corresponding histology (J). K) OCT image of normal lymph node tissue demonstrating the follicles (i) capsule (ii), and fat on the external surface (iii). L) Corresponding histology of normal lymph node tissue also demonstrated follicles in the cortex, with a pale center and

a dark rim (i), a fibrous capsule (ii), and surrounding adipose tissue (iii). M) OCT image of normal adipose tissue with the corresponding histology (N). OCT image scale bar is represented. Histology images are at 100x magnification.

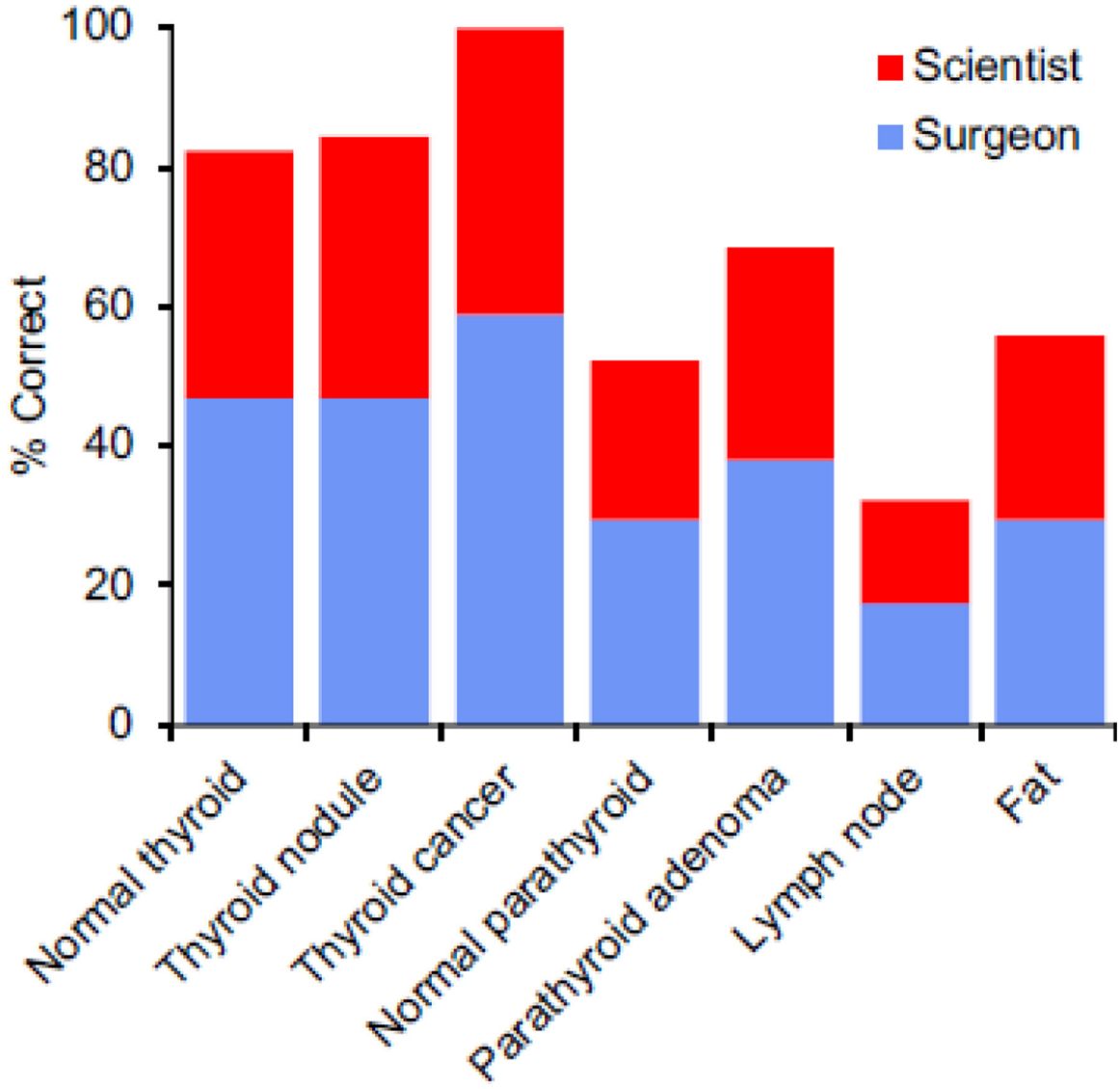

Figure 4.
Correct identification of tissue type amongst surgeons and scientists combined.

Table 1.

OCT optical appearance by tissue type

Tissue	OCT Optical Appearance
Normal Thyroid	Thin, high light scattering capsule. Subcapsular follicle bearing tissue with low signal intensity.
Thyroid Nodule	Thick high light scattering capsule. Subcapsular follicle bearing tissue with low signal intensity.
Thyroid Cancer	Thick, highly light scattering capsule. Subcapsular tissue of low intensity. No follicles.
Normal Parathyroid	Thin, highly light scattering capsule Subcapsular homogenous tissue. Regions of no signal intensity.
Parathyroid Adenoma	Thin, highly light scattering capsule. Subcapsular homogenous tissue with fewer regions of no signal intensity.
Lymph Node	Thin, highly light scattering capsule. Subcapsular homogenous tissue that fades.
Fat	High light scattering honeycomb-like pattern surrounding regions of no signal intensity.

Table 2.

Correct identification of tissue type between surgeons and scientists

		No. correct (%)		
OCT Image	**No. images per survey**	**Surgeon n=10**	**Scientist n=7**	**p-value**
Normal thyroid	3	24 (80.0%)	18 (85.7%)	0.7197
Thyroid nodule	3	24 (80.0%)	19 (90.5%)	0.4448
Thyroid cancer	3	30 (100.0%)	21 (100.0%)	1.0000
Normal parathyroid	10	50 (50.0%)	39 (55.7%)	0.5332
Parathyroid adenoma	9	58 (64.4%)	47 (74.6%)	0.2169
Lymph node	2	6 (30.0%)	5 (35.7%)	1.0000
Fat	2	10 (50.0%)	9 (64.3%)	0.4953